

Luminescence of phosphorus doped silica glass

A.N. Trukhin^{a, 1}, A. Antuzevics^a, K. Golant^b, D.L. Griscom^c

^a Institute of Solid State Physics, University of Latvia, LV-1063 Riga, Latvia

^b Institute of Radio-engineering and Electronics, RAS, 125009 Moscow, Russia

^c Impact Glass Research International, 3938 E Grant Rd #331, Tucson, AZ 85712, USA

abstract

A fiber preform with P-doped silica core is studied by luminescence methods. P-doped silica was synthesized via the SPCVD method on a substrate tube made of pure silica glass F300. Two luminescence bands were detected under excitation of the F₂ excimer laser (157 nm). One band is in UV range at 4.6 eV (265 nm) with two time constants ~30 ns and 5 μs and the other at 3.1 eV (400 nm) with time constant ~5.5 ms. Fast decay of the blue band with time constant ~20 ns was also observed. The main excitation band of the UV luminescence is at 7.1 eV (~170 nm) and that for blue band is at 6.3 eV (~195 nm). These bands belong to two different luminescence centers, however, both are associated with the presence of phosphorus. The UV band is similar to the one observed in many different oxide materials containing phosphorus and is ascribed to PO³₄⁻ complex ion. The blue band is ascribed to a twofold coordinated phosphorus. Both the blue and the UV luminescences participate in the recombination process due to electron trapping. These luminescences appear due to thermal stimulation upon recombination of liberated self-trapped holes. Other than the detected phosphorus-related oxygen-hole-centers, there is no other recombination luminescence.

1. Introduction

Phosphorus is one of the dopants in silica glass changing the index of refraction in order to adjust the properties of optical fibers. On the other hand, phosphorus is interesting for codoping ions in many materials, thus useful for fundamental research. Phosphorus takes on a variety of valence states in different oxides doped with phosphorus. The phosphite ion PO³₃⁻, the orthophosphate ion PO³₄⁻, and the pyrophosphate ion P₂O⁴₇⁻ are among them. Also intriguing could be phosphorus mon-oxide, as well as the PO₂. These ions determine various phenomena in those oxides. It is found that the PO³₄⁻ complex is the main structural element in silicon dioxide doped with phosphorus [1].

Phosphorus gives its name to one kind of luminescence – phosphorescence - thus it is natural to study properties of phosphorus doped materials by luminescence methods.

Analyses of literature related to the luminescence of different materials with phosphorus (e.g. [2,3]), show that the common luminescence property of these materials is the observation of a UV band. Thus, in ScPO₄ zircon-type crystal the band at 5.7 eV is interpreted as self-trapped exciton (STE) of this crystal [2]. AlPO₄ and GaPO₄, both with structure of α-quartz, give rise to the UV bands situated at 5.83 eV and 5.65 eV respectively, and are thus interpreted as the second STE

related to orthophosphate ions [2]. The first STE is similar to that of α-quartz, which band is situated in the visible range of the spectrum. In phosphorus-doped crystalline α-quartz, phosphor-silicate glass, and lime phosphate glasses, the UV bands are situated at 4.9 eV; 4.8 eV; 4.1 eV respectively [3]. These bands are interpreted as luminescence of phosphorus related defects in the corresponding structure. In all the cases the UV band exhibits relatively fast decay in ns range of time, ascribed to singlet-singlet transitions with decay times of tens of μs due to triplet-singlet transitions. A model for the UV luminescence center is assumed on the basis of the STE in ScPO₄, where the hole component is situated on orthophosphate and the electron component is dispersed around scandium. Mentioned materials have differing properties. ScPO₄ is a dry crystal, whereas a phosphorus-doped crystalline quartz sample was found to contain about 3400 atomic ppm of water and OH groups. However, the existence of UV luminescence does not depend on water content.

Another situation is the non-UV band luminescence in the mentioned materials. In ScPO₄, huge amounts of different luminescence bands were observed (see e.g. [4]), mainly related to impurities.

The luminescence of phosphorus doped crystalline quartz sample exhibits yellow-red bands at 600 nm (2.065 eV) and 740 nm (1.65 eV). Corresponding centers are created by excitation light. A similar yellow luminescence was observed for 3P₂O₅·7SiO₂ glass [3]. However, in Ref. [5] silica glass fiber preforms with phosphorus in the core do not exhibit such yellow luminescence. Instead, there is a blue luminescence with a time constant of about 6 ms was observed. It is

necessary to underline that this blue luminescence was mainly observed under excitation with a UV laser. In Ref. [5], there was also an attempt to measure photoluminescence excitation spectra excited by synchrotron light. However, observation was made on a total slice of preform including the cladding. So, it is not certain that the excitation spectrum corresponded to P-doped core.

So, in this work we have performed studies of luminescence in phosphorus-doped silica glass obtained by chemical vapor deposition (Surface Plasma Chemical Vapor Deposition). Material obtained through this method contains very little water or OH groups. In that regard, it is different from previously studied materials [3]. As for previous samples, we have compared a UV luminescence with similar properties. However, yellow-red luminescence was not observed at all. Instead, we observed blue luminescence with long duration kinetics, as was antecedently discovered in [5].

Blue luminescence related to phosphorus was observed in KCl-P crystals [6]. It is remarkable that the slow decay (a few ms) of this blue luminescence has been observed, as in the case of Ref. [6]. PO_2^- is responsible for blue luminescence in KCl-P crystal. Finally, we came to the conclusion that similar defects could be responsible for blue luminescence in silica glass with phosphorus. However, in Ref. [5] the blue luminescence was ascribed to a defect consisting of diamagnetic four-coordinated P impurity substitutional for a Si atom.

2. Experimental procedure

The SPCVD sample was a fiber preform 10 mm in diameter. The pure silica glass (Suprasil F300) tube was used for deposition of phosphorus containing pure silicon dioxide (see Ref. [7]). After deposition the tube was compressed at high temperature and two preforms with P-doped core were obtained. The concentration was about 1% of P_2O_5 . One core was 4 mm in diameter and the other was 2 mm. Slices of different thickness were made: 0.4 mm, 1 mm and 5 mm. Diaphragms were used that avoid excitation of cladding, which were made from pure silica. The profile of the index of the preform is presented in Fig.1.

The photon counting mode instrumented with the Hamamatsu H8259-02 module was used for slow luminescence detection. Inside the module beside the PM there were an amplifier, comparator, and a pulse former. This mode was used for low intensity luminescence. Fast intensive luminescence was detected by PMT Hamamatsu H6780-04 in current regime. There PM anode is loaded with a 50 Ohm resistor. Luminescence decay curves were recorded by a Tektronics TDS 2022B oscilloscope, each curve being averaged over 128 pulses. The time-resolved luminescence spectra were extracted from the decay curves measured at each specific wavelength. The corresponding decay curve was integrated within a measured time interval. The ArF (193 nm

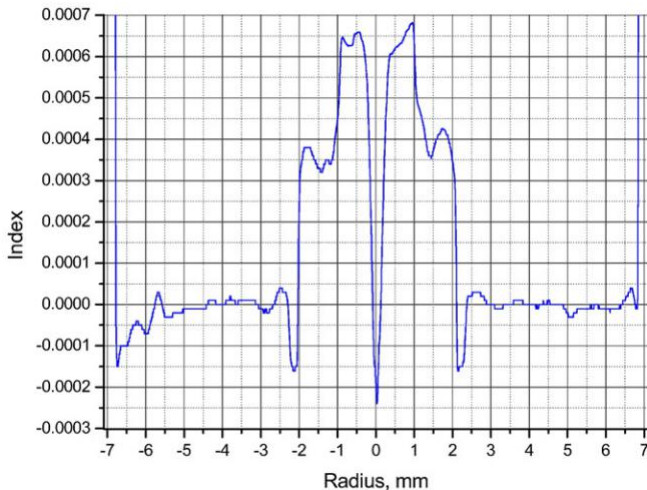


Fig. 1. Profile of index of the preform $P_2O_5:SiO_2$ 1 mol% - $n \sim 0.001$.

wavelength) and KrF (248 nm wavelength) excimer lasers, model PSX-100 of Neweks (Estonia) with pulse energy of up to 5 mJ and pulse duration of 5 ns were used to excite the luminescence. Also, a ten-times less powerful F2 laser (157 nm) was used. Luminescence emission was collected in a direction perpendicular to the excitation laser beam. The samples were carefully cleaned and mounted on a holder; no glue was used. Measurements were performed at 60–350 K sample temperatures. The lower temperature of 60 K was obtained by pumping of liquid nitrogen from cryostat. Some measurements were performed on a helium refrigerator in the range of temperature 10–290 K. The high temperature range was checked in a sample holder with heating.

Luminescence was detected with the help of a grating monochromator (MCD-1) with slit width of about 1 mm corresponding to 1.5 nm spectral resolution. The measured curves are mainly presented in the figures as recorded; therefore, they reflect the level of errors. Very noisy curves were smoothed by a sliding average approach. Also, the life time of the gas in the excimer laser was short, with intensity deteriorating with time. However, frequent changing of the gas is costly, so we tried to perform measurement in time when detectable luminescence could be recorded. Then comparison of intensities within one figure is guaranteed, whereas long-time correspondence related to different presented figures was difficult.

3. Results

3.1. Optical properties

The optical absorption spectrum of the P-doped core of preform is presented in Fig.2. When measuring a 4 mm thick sample we detected well resolved bands at ~ 6.8 to 7.0 eV and at ~ 7.3 to 7.5 eV. The optical gap is situated at 8.1 – 8.2 eV and it is well correspondent with known properties of pure silica position of the optical gap (see e.g. [8]). A 0.4 mm thick sample was used for analyses of the absorption spectrum near optical gap, Fig.2 insert. For pure silica, the optical gap obeys the Urbach rule, explained by Toyozawa [9] as a momentary self-trapped exciton (STE) creation similar to that of α -quartz crystal. The properties of the pure silica optical gap can be found in [8,10]. A remarkable property is the crossing of all spectra in semi-log scale at one point. However, for phosphorus-doped core silica, the obtained spectra for different temperatures on a semi-log scale exhibit parallel shifts with temperature, Fig.2 insert. This case is known for disordered materials. The

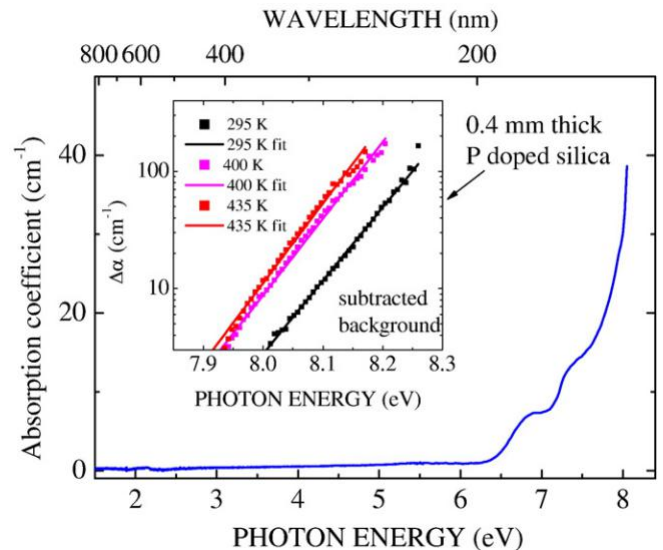


Fig. 2. Optical absorption spectra of silica preform with P-doped core, 4 mm thick sample. Insert – absorption spectra at different temperatures for 0.4 mm thin sample (points). Lines – fit to expression (1) of glass-like Urbach rule for optical gap.

intrinsic absorption obeys the Urbach rule in the usual form for disordered materials [11,12]:

$$\alpha \propto I_0 \exp \left[\frac{1}{2} A E \right] \exp \left[-\frac{E}{T_1} \right]$$

where A is a parameter of the slope, T_1 is a characteristic temperature, and E is the photon energy and I_0 is fitting parameter. The slope coefficient $A = 15 \pm 1 \text{ eV}^{-1}$ and the characteristic temperature $T_1 = 18 \pm 3 \text{ K}$ are determined for the case of the P-doped-core sample as $I_0 = 5.1 \cdot 10^{-60} \text{ cm}^{-1}$ or ($I_0 = \exp(-138.9)$).

Optical absorption of a 5-mm-thick sample is presented in Fig.3a. There are several bands in the core. After irradiation of the core subjected to ArF laser light, the band at 2.24 eV increases. In Fig.3b the absorption spectrum of the P-doped core of the fiber preform is compared with the photoluminescence excitation spectra. However, the PL excitation takes place in the range of absorption bands that are not in direct correspondence with the excitation band maxima. Perhaps those absorption bands are not resolved on the background. Moreover, the intensity of photoluminescence excited through vacuum monochromator with low power deuterium discharge source is low and the PLE curves are noisy. The presented PLE spectra are smoothed by a sliding-least-squares approach. The PL spectra are measurable more precisely with excitation by excimer lasers, which do not need smoothing for presentation. The photoluminescence bands measured under laser excitation are also presented in Fig.3b. The photoluminescence and its time constants for the spectra of a P-doped-core silica fiber preform detected in different ranges of time are presented in Fig.4. There is also a band

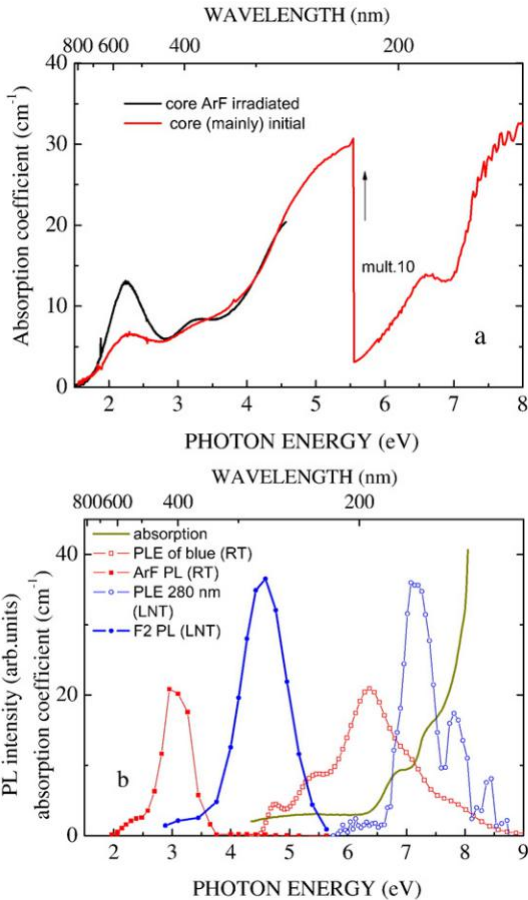


Fig. 3. (a) Optical absorption of 5 mm sample of silica preform with P-doped core. Part below 5.5 eV is increased 10 times. Irradiation of core with ArF laser provides growth of a band at 2.24 eV. (b) Comparison of optical absorption spectrum with photoluminescence excitation spectra (PLE). Smoothing of PLE spectra by sliding least-squares approach was made. The PL bands measured under excimer lasers excitation are presented.

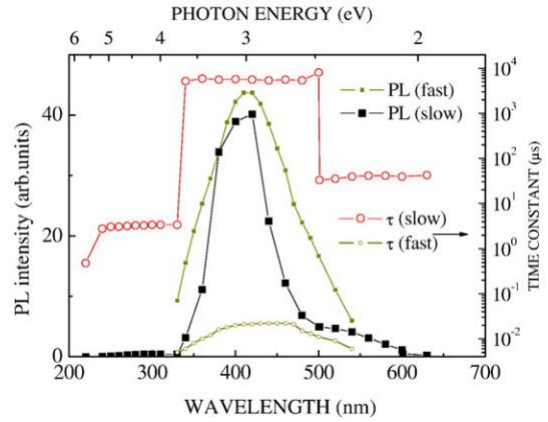


Fig. 4. PL (square) and τ (circles) spectra of P-doped silica ArF, 293 K. Small points for fast decay, big points for slow decay. The lines are to guide the eye.

at 400 nm with time constant 5.2 ms and smaller band at 600 nm with a time constant about 40 μs (Fig.4). The band at 400 nm also possesses a fast decay $\sim 20 \text{ ns}$. The corresponding PL band is a bit broader than the band with slow decay. There is also the same PL band at 300 nm with a decay time in the μs range. It is seen that the band at 400 nm possesses an almost uniform distribution of time constants from 5 ms to 6 ms. The decay kinetics is an exponential (which is rare for glassy materials) after the fast peak seen in Fig.5. The decay duration is not changed with cooling. The intensity of the band at 400 nm also changes little with cooling from 293 K to 80 K Fig.5. Also in Fig. 5, we have studied the polarization properties of the time-resolved blue luminescence of the P-doped core under excitation with KrF laser through a polarizer made from three gold coated mirrors. The polarization degree was determined as $P = (V \setminus H) / (V + H)$, where V is intensity of luminescence for analyzer parallel to electric vector and H is perpendicular to that. We found that the blue luminescence is negatively polarized with respect to excitation electric vector direction. The degree of polarization is practically independent on temperature. All curves of decay in Fig.5 are normalized to the maximum in initial stage of decay, and their difference does not show a slow luminescence intensity thermal dependence. As mentioned above, the intensity changes little with cooling.

In the high temperature range, Fig.6, the intensity of the blue luminescence and the decay time constant possess similar temperature dependences. Its PL $I(T)$ and $\tau(T)$ approximate Mott's law [I or $\tau = I_0$ or $\tau_0 / (1 + f \cdot \tau_0 \exp(-E / kT))$], thus providing thermal quenching activation energy $E = 0.5 \pm 0.05 \text{ eV}$ and frequency factor $f \sim 10^9 \text{ s}^{-1}$.

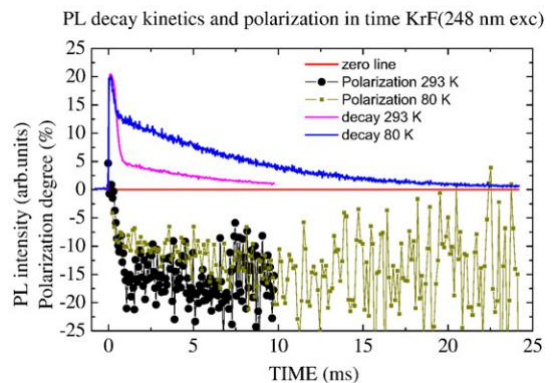


Fig. 5. The example of decay kinetics obtained under KrF laser. Time resolved blue luminescence polarization determined as $P = [(V \setminus H) / (V + H)] \cdot 100$, V – decay kinetics for parallel and H – for perpendicular analyzer with respect to excitation electric vector. So, luminescence electric vector is oriented orthogonally to excitation electric vector.

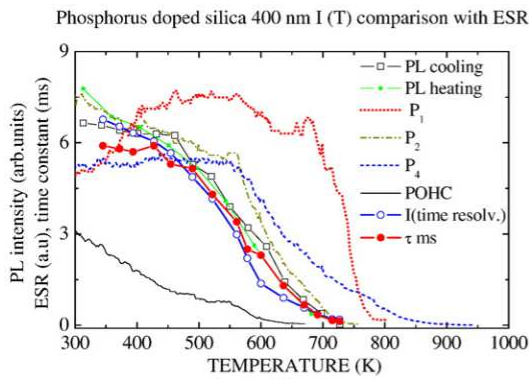


Fig. 6. Thermal dependences of 400 nm PL, τ and I, of phosphorus doped silica under ArF excitation. Points connected by straight lines. PL I(T) and $\tau(T)$ approximation with Mott's law [I or $\tau = I_0$ or $\tau_0 / (1 + f \cdot \tau_0 \exp(-E / kT))$] provide thermal quenching activation energy $E = 0.5 \pm 0.05$ eV and frequency factor $f \sim 10^9 \text{ s}^{-1}$. The curves marked P1, P2, P4 and POHC are ESR data from [1] presented for comparison.

Therefore, these two values are determined by intra center quenching processes.

Although PL is the principle purpose of this paper, Fig. 6 actually represents the number density of radiation-induced phosphorous defects created at 300 K and subsequently annealed as functions of increasing temperature. Here, thermal quenching of the PL parameter dips from 300 K to virtually nothing at 750 K but it can be reversed without loss upon cooling. In Fig. 6 the P1, P2, P4, and POHCs defects are recorded in the range 300 to 750 K. These data employ the same nomenclature as that evolved in fig. 12 of Ref. [1]. However, the latter was measured from 100 K upward, rather than from 300 K, and it extends to 1150 K. But for present purposes, the data of fig. 12 of Ref. [1] will be truncated at 560 K. So, from 100 K to 560 K, P2 is dominant and decreases only ~8% upon reaching 560 K. P2 is known to be a four-coordinated phosphorus atom that has trapped an electron. Thus, all of the rest are trapped hole centers. P4 is found to move nearly horizontally as the temperature rises from 100 to 560 K. In contrast, P1 grew linearly before flattening out at ~400 K, and in the same range, the POHC moved downward at the a slightly increasing rate after crossing P1 at 200 K.

In addition, Ref. [1] reported a defect that appeared close to P1 at 100 K, but from there dived steeply downward nearly two orders of magnitude by 300 K. This feature was noted by the authors of [1], who finally decided that it was a type of E' center which they dubbed "Si E' (P)" because of its narrowness and lack of hyperfine doublets, as

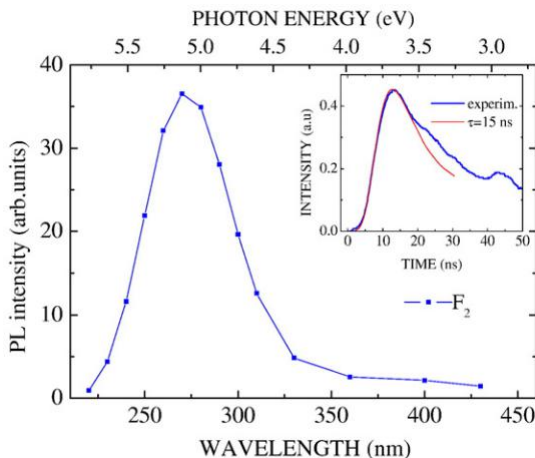


Fig. 7. Time resolved (ns) PL spectra and, insert, decay kinetics of UV band under F2 laser. Time constant τ was determined by fastest fit of laser pulse convoluted with exponent with time constant 15 ns. Discrepancy in higher time shows on existence also of component of decay with higher time constant T-80 K.

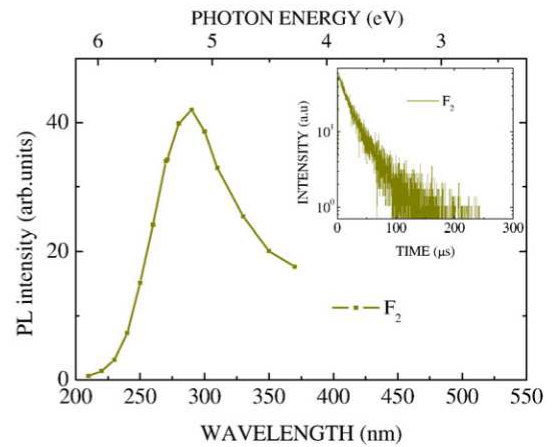


Fig. 8. Time resolved PL spectra in the range of 100 μs . Insert presents decay kinetics of UV band under F2 laser.

would be expected for phosphorous bearing entities. However, 7 years later Griscom discovered self-trapped holes in silica glass [13], later proved it in detail [14], and finally added additional thoughts in [15, 16]. In [15] it is found that solid evidence that the "Si E' (P)" found at the low temperature end of x-irradiated P2O5-SiO2 K [1] had nothing at all to do with phosphorus; rather it was the work of self-trapped holes!

The time resolved PL spectrum in Fig.7 (main part) and decay kinetics (insert) of the UV band are due to F2 laser excitation. The data of Fig.7 were recorded with the PM in the current regime. In the insert to Fig. 7, an exponential approximation reveals the main decay time constant of 15 ns. Evidently the decay is non-exponential and there is a long duration time as seen in the insert. In Fig.8 the time resolved PL spectrum excited with F2 laser light is presented. The intensities at different points are determined by integration of the decay curves measured with a photon-counting method. An example of this curve is presented in the Fig.8, insert. The duration was about 100 μs .

In Fig.9 the UV PL spectra are compared with both the ns and μs time ranges under F2 laser at 77 K. The shift of the slow duration PL band at the lower photon energy with respect to the fast duration PL band should be noted. For this reason we interpret it as a manifestation of singlet-triplet splitting. Therefore, we ascribe the slow UV band to triplet-singlet transitions and the fast UV band to singlet-singlet transitions of

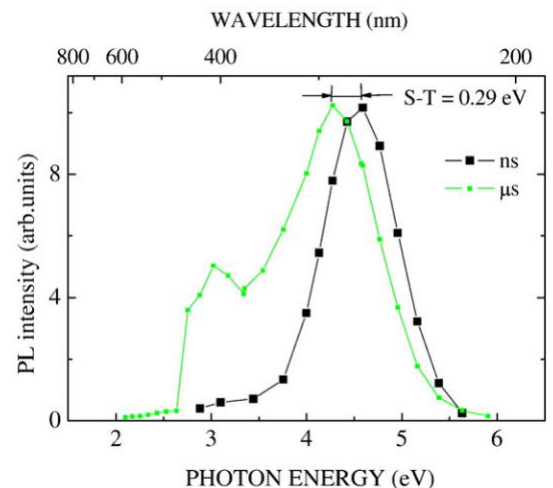


Fig. 9. Comparison of UV PL spectra of P-doped silica preform core measured in the ns and hundreds of μs time range under F2 laser at 77 K. Mutual shifts of the bands on 0.29 eV could witness on singlet-triplet splitting of excited state of the luminescence center.

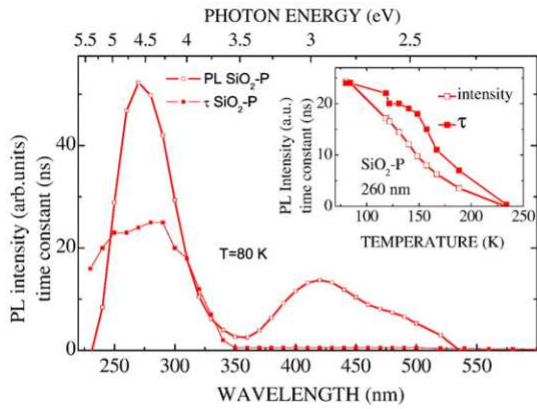


Fig. 10. Time resolved PL and time constant spectra of SiO₂-P under F₂ laser. Insert PL intensity and time constant temperature dependence for 260 nm band. Time constant τ was determined analogously to Fig.8, however longest duration was taken. Intensity thermal dependence exhibits exponential growth with cooling usual for disordered materials.

P related luminescence center. The shoulder at 3 eV is evidently a blue band, the data for which are presented above.

The spectral distribution of the decay kinetics of the UV luminescence of SiO₂-P glass is provided in Fig. 10 for both PL SiO₂-P and τ SiO₂-P as functions of both wavelength (main figure) and temperature (insert). Of extreme interest is the fact that the lower of the two curves of the insert matches very well STH₂ in that range while the higher curve of the insert matches well STH₁, as clearly shown in fig. 7 of [15].

3.2. Radiation properties

In Fig.11 the luminescence spectra for x-ray and F₂ laser excitation are compared. The UV band could also be excited in the thermally stimulated luminescence (TSL) regime, insert Fig.11. TSL contains several peaks in the range 100–200 K. Also, the band at 400 nm could be seen in TSL with a different shape, i.e., having one main peak at 120 K. However, the band at 270 nm (the green curve) does not behave as TSL upon ArF laser excitation, heading downward, whereas the TSLs all started at zero and headed up. Indeed, during steady state excitation with x-rays, the intensity of the band at 270 nm increases with cooling, Fig.11, I(T) insert.

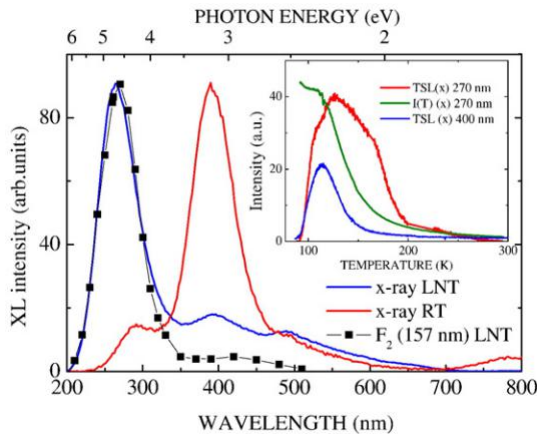


Fig. 11. Luminescence spectra of P-doped core of silica fiber preformed under excitation of F₂ laser (157 nm) and x-ray at 293 K and 80 K. The spectra are measured differently and so were scaled so as to fit both on the same graph. Insert – thermally stimulated luminescence for different bands after x-ray—as well as the temperature dependence of the x-ray-created 270 nm band, which is almost certainly due to self-trapped holes; see [13–16] and discussion at the end of Section 3.1. No TSL was detected after ArF laser irradiation of annealed at 700 C samples.

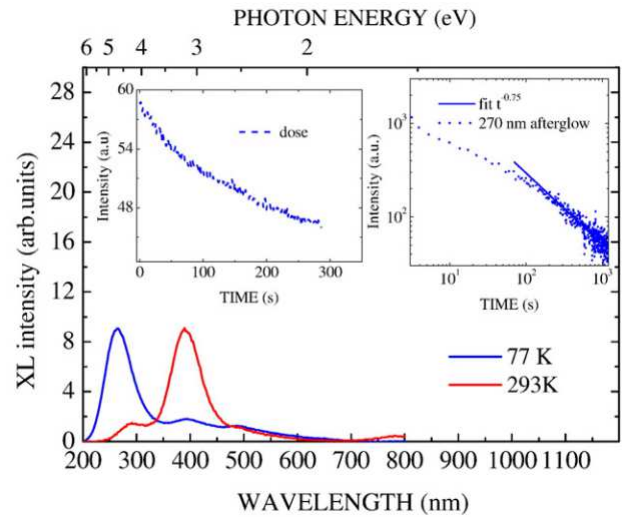


Fig. 12. X-ray excited luminescence spectra of silica with phosphorus at 293 K and 80 K. Left insert: Dose dependence during x-ray irradiation. Right insert: afterglow kinetics curve of P-doped silica fiber preform. Line is approximation of afterglow with $t^{-0.75}$.

In Fig.12, the dose dependence during x-ray irradiation and the afterglow kinetics curve are presented as the left and right inserts, respectively. The decrease of 270 nm luminescence intensity during irradiation shows that the corresponding luminescence center participates in charge trapping and therefore the quantity of emitting centers is decreased. The afterglow shows that there is a recombination of

trapped charge carriers. The kinetics could be approximated by the law $t^{-0.75}$ in the end of afterglow. This may be explained by tunneling recombination of closest pairs of electrons and holes. It is known [17] that tunneling recombination possesses characteristic t^{-1} law. Our value $t^{-0.75}$ is close to that. N.B. The abscissa recapitulates that of Fig. 11.

Our electron spin resonance (ESR) spectra of P-doped core of a silica fiber preform are shown in Fig.13. This sample was initially annealed at 1000 K, then cooled to 77 K, irradiated with x-rays, and an ESR spectrum was recorded. Subsequently, the sample was heated to 293 K and kept at that temperature 20 h, then we recorded the spectrum again. The insert on the right shows dose dependence of signal intensity at 77 K. The insert on left shows the DPPH spectrum (reference materials with $g = 2$). The interpretation of the obtained ESR spectra is based on literature data. Specially, the spectrum of 293 K at the top corresponds to the well-known doublet signal of the Phosphorus Oxygen Hole Center (POHC)

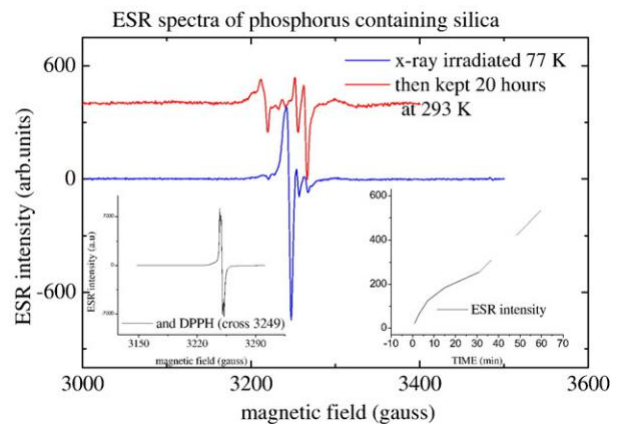


Fig. 13. Study of electron spin resonance (ESR) spectra of P-doped core of silica fiber preform subjected to x-ray irradiation. (No signal is seen before irradiation.) The irradiated sample was initially annealed at 1000 K, then cooled to 77 K and measured ESR spectrum (blue curve). Then the sample was heated to 293 K and kept at that temperature 20 h. Insert on right shows dose dependence of signal intensity at 77 K as a function of time. Insert on left shows DPPH spectrum (reference materials with $g = 2$).

[1] where, in the present case, the weak off-center peak is due to silicon E' centers (similar to fig. 2 insert of [16]). The spectrum obtained by x-ray irradiation at 77 K also includes weak POHC and E' signals. However, the principle 77 K spectrum (blue at bottom) corresponds well with self-trapped holes (STHs) created at that temperature (see [13–16]). During heating toward room temperature those STHs are liberated as free holes (see last paragraph of Section 3.1, above), which in the present case combine with P₂O₅ units in silica glass, thus creating the POHCs (i.e., 2-coordinated phosphorus atoms that trap a hole) see [1]. In addition, some liberated holes recombine with trapped electrons to create TSL peaks (Fig.11) and afterglow (Fig.12, right insert).

In Fig.14 the influence of ArF laser irradiation on our ESR samples is shown. The sample was initially annealed at 1000 K, then cooled to 77 K, irradiated with pulses of ArF laser, and finally recorded as an ESR spectrum. Then the sample was again annealed at 1000 K, cooled to 293 K, irradiated with pulses of ArF laser, and finally measured again by ESR. The insert on right of Fig. 14 shows the ESR spectrum of an E'-center in the ArF irradiated cladding (i.e., part of sample without phosphorus). In the case of irradiation with photons of an ArF laser, contrary to the case of x-ray irradiation, a POHC signal is also created at 77 K, whereas irradiation with pulses of ArF laser at 293 K also creates a POHC signal.

4. Discussion

We have observed two main luminescence bands. One is in the UV range with maximum at about 270 nm and a blue, and another at 400 nm. Both bands are related to the presence of phosphorus in silica glass. We did not find mutual influence of the corresponding luminescence centers. Therefore, these centers are attributed to different structural defects in silica-glass-containing phosphorus. The slow decay of the blue band is about 6 ms, little depending on temperature up to 500 K. Beside the slow component, a fast component of blue-band decay is also observed in Fig.4. The time-resolved PL band for the fast component is situated at 400 nm as well. However, it is broader; see Fig.4. Thermal quenching of blue luminescence takes place above 500 K with activation energy $E = 0.5$ eV and frequency factor $f \sim 10^9$ s⁻¹ Fig.6. Thermal dependences of PL (Fig.6) show good correspondence between PL intensity and the slow decay time constant. This could mean intra-center quenching of the blue luminescence center. Comparison of PL thermal dependences with that of the ESR-studied self-trapped holes in silica glass [13–16] shows that PL-center quenching does not directly correlate with annealing of radiation induced P₁ centers (radiation induced holes trapped on a three-coordinated phosphorous ions) [1]. However, PL thermal dependence is close to

that of the P₂ center (a 4-coordinated P that has captured an electron [1]) and P₄ centers (2-coordinated P that has trapped an electron [11]). However, there are remarkable differences.

The case of KCl-P crystal [6], where blue luminescence possessing decay with $\tau = 2$ ms (also $\tau = 90$ ms was detected there as well), was studied here in detail, and the molecular center O-P-O (i.e., P₄ [1]) was deduced. That could also be an argument in favor of such a center being created in silica glass with phosphorus, where the electronic transitions are certainly triplet-singlet, as it was interpreted in [5]. In [6] the KCl-P crystal, the natural triplet state and the allowance of the triplet singlet transition by spin-orbit coupling was ascribed to states of oxy-gen. P-doped silica is ascribed to a triplet-singlet transition, and the fast decay of the blue band is ascribed to singlet-singlet transition [3]. Similar positions of time-resolved bands exhibit low-value singlet-triplet splitting of the excited state of the center. That means that the corresponding wave function is spread in space.

Another known case of two-fold coordinated centers in silica is SiODC(II) and GeODC(II). For the latter center, a remarkable characteristic is the high value of singlet-triplet splitting of corresponding excited states [18]. The triplet-singlet band is situated at 450 nm (2.6 eV) for SiODC(II) and at 395 nm (3.1 eV) for GeODC(II). The singlet-singlet PL bands are situated at 280 nm (4.4 eV) and 290 nm (4.3 eV) correspondingly. So, the singlet-triplet splitting of excited states is about 1.8 eV and 1.2 eV. A large singlet-triplet splitting corresponds to a wave function localized in small space. So, in the case of the P-related two-fold coordinated center in silica, termed P₄ if it had captured a hole, it is different and corresponds better to two-fold coordinated center in KCl-P [6]. There, the wave function of the excited state is spread in space, and the spin-orbit coupling constant allows a triplet-singlet transition related to oxygen atoms, whereas in the cases of SiODC(II) and GeODC(II) the singlet-singlet transition [18] is related to Si or Ge.

The previous cases include a quartz crystal with phosphorus and a phosphosilicate glass, where blue luminescence related to phosphorus was not observed. This could be explained by presence of water and/or OH groups in these materials [3]. However, an actual sample of silica with phosphorus was found to be practically free of such contamination.

The intensity of UV luminescence of P-doped silica is also seen both under low intensity excitation such as deuterium discharge light source and excimer lasers. Previously we had observed the UV band in different phosphate crystals and glasses (see e.g. [2,3]). The UV band decay kinetics is fast (~30 ns), whereas there is also a slower component in the μ s range of time. This situation takes place in all the cases. However, there are differences depending on excitation conditions in different materials.

Possibly, such UV luminescence is a general property of orthophosphates. Observation of the band at 210 nm after soldering [3] by use of orthophosphate acid is an argument for that. In the case of the ScPO₄ crystal, the UV band at 210 nm possesses a fast component (30 ns) and slow components (~10 μ s), which were interpreted as singlet-singlet and triplet-singlet transitions of the self-trapped exciton [2,4]. The STE in ScPO₄ is ascribed to the PO₃⁴⁻ molecular ion. In the case of crystal-line quartz doped with phosphorus it was found that this UV band consists of two components of decay (~30 ns and ~10 μ s, see Ref. [3]). However, the UV band in quartz is situated at ~250 nm, and was ascribed to PO₃⁴⁻ molecular ion as well. Presumably different surroundings of PO₃⁴⁻ molecular ion in the quartz and orthophosphate of scandium explain the differences in band position. Similar interpretations of the UV band in other phosphates have been made [2–4]. So, in the actual case, the UV band in silica glass with phosphorus could be explained in a similar way. That is, based on observation of two components of decay, one fast and one slow, in the mentioned materials. The data presented in Fig.9 are interpreted as singlet-triplet splitting of the excited state of the center with a value of splitting equal 0.29 eV. This is remarkably higher than that of the blue luminescence center.

The UV band thermal dependences are similar to the presently studied silica glass with phosphorus and the previously studied quartz

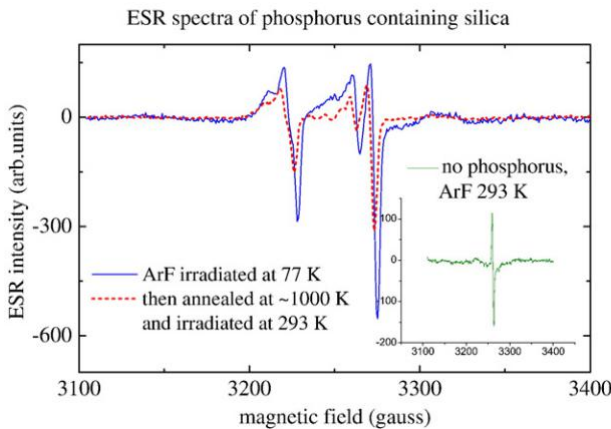


Fig. 14. ESR spectra of P-doped core of silica fiber preform. Sample was initially annealed at 1000 K, then cooled to 77 K, irradiated with pulses of ArF laser and measured ESR spectrum. Then the sample was again annealed at 1000 K cooled to 293 K and irradiated with pulses of ArF laser, then measured spectrum. Insert on right shows ESR spectrum of ArF irradiated cladding (part of sample without phosphorus).

crystal doped with phosphorus [3], Fig.10. The decay in the crystal is faster (15 ns) at 8 K whereas in silica glass with P decay it is about 30 ns.

We did not find a correlation between the center of the UV and that of the blue luminescence, with the exception that both are due to presence of phosphorus. This could be explained as due to the multivalent property of phosphorus-related defects in various matrices. Phosphorus takes on a variety of valence states in different oxides doped with phosphorus. The phosphate ion PO_3^{3-} , the orthophosphate ion PO_4^{3-} , and the pyrophosphate ion $\text{P}_2\text{O}_7^{4-}$ are among them [1]. These ions determine different phenomena in P-doped materials. It is clear that the PO_4^{3-} complex is the main structural element in silicon dioxide doped with phosphorus below 600 K [1]. The similarities of the properties of the UV band in silica glass and that in ScPO_4 suggest that the UV band in all phosphorus-containing materials may be dominated by the PO_4^{3-} complex. However, the blue band is also ascribed to this element [5]. Thus the problem needs further investigations. Two slightly differing bands are observed in thermally stimulated luminescence after x-ray irradiation at LNT and RT of silica glass with phosphorus Fig.11. However, there is some difference in TSL curves for UV and blue luminescence supporting the absence of mutual dependence of these centers. Decrease of the UV band with a dose of irradiation implies the destruction of the luminescence center, presumably by trapping of a charge carrier. The afterglow (Fig. 12) witnesses the existence of a recombination process of this trapped charge with carriers of another sign.

5. Conclusions

UV luminescence is provided by a center existing in as-received materials and ascribed to the states related to PO_4^{3-} ion based on the similarity of this UV luminescence with STE luminescence in ScPO_4 . The blue luminescence is negatively polarized when excited with polarized light. Upon warming, both luminescence bands appear in

recombination of liberated self-trapped holes with the electron trapped on differing phosphorus related structures. One is in the UV luminescence center and the other for blue luminescence center. The first is ascribed to PO_4^{3-} and the second is likely twofold coordinated phosphorus (O-P-O). We did not find luminescence due to electron recombination with POHC.

Acknowledgements

This work is supported by Material Science program IMIS2 of Latvia.

References

- [1] D.L. Griscom, E.J. Friebele, K.J. Long, J.W. Fleming, *J. Appl. Phys.* 54 (1983) 3743.
- [2] A.N. Trukhin, K. Smits, J.L. Jansons, L.A. Boatner, *J. Phys. Condens. Matter* 25 (2013) 385502 (6pp).
- [3] A.N. Trukhin, K. Smits, J. Jansons, D. Berzins, G. Chikvaidze, D.L. Griscom, *AIP Conference Proceedings*, 1624, 2014 154.
- [4] A.N. Trukhin, L.A. Boatner, *Proceeding of the 13 IC Defect in Insulating Crystals*, 239–241, Material Science Forum, Wake Forest University, 1996 573.
- [5] G. Origlio, F. Messina, M. Cannas, R. Boscaino, S. Girard, A. Boukenter, Y. Ouerdane, *Phys. Rev. B* 80 (2009) 205208.
- [6] S.J. Hunter, K.W. Hipps, A.H. Francis, *Chem. Phys.* 39 (1979) 209–220.
- [7] K.M. Golant, in: G. Pacchioni, L. Skuja, D.L. Griscom (Eds.), *Defects in SiO_2 and Related Dielectrics: Science and Technology*, Kluwer Academic, London 2000, p. 427.
- [8] I. Godmanis, A. Truhins, K. Hubners, *Phys.Stat. Sol. (b)* 116 (1983) 279.
- [9] Y.A. Toyozawa, *Techn. Report. ISSP A1* (1964) 119–168.
- [10] A.N. Trukhin, *J. Non-Cryst. Solids* 149 (1992) 32.
- [11] L. B. Glebov, (Ph.D thesis), University of Leningrad (1975) 22.
- [12] B.L. Gelmont, V.I. Perel, I.N. Jassievich, *Sov Solid State Physics* 25 (1983) 727.
- [13] D.L. Griscom, *Phys. Rev. B* 40 (1989) 4224.
- [14] D.L. Griscom, *J. Non-Crystalline Solids* (1992) 137.
- [15] D.L. Griscom, *J. Non-Crystalline Solids* (2004) 139.
- [16] D.L. Griscom, *J. Non-Crystalline Solids* (2006) 2601.
- [17] A.R. Kangro, M.N. Tolstoi, I.K. Vitols, *J. Lumin.* 20 (1979) 349.
- [18] L.N. Skuja, *J. Non-Cryst. Solids* 239 (1998) 16.